simple with no evidence for either magnetic or chemical nonequivalence of the fluorine bonded to sulfur. However, when $R_f = R_f' = C_2F_5$, the spectrum is much more complex and has not been completely interpreted.

The SF chemical shifts of known R_fSF_3 and $R_fR_f'SF_2$ compounds are given in Table I. Muetterties et al.[6] have argued that because the observed resonance of $R_fR_f'SF_2$ compounds is intermediate between the axial and equatorial positions of the R_fSF_3 compounds, a rapid axial–equatorial exchange may be occurring in the $R_fR_f'SF_2$ compounds. By contrast, intermolecular exchange of axial (but not equatorial) fluorine atoms is suggested for SF_4[9] and was extended by Seel[10] to other three- and four-coordinated sulfur(IV) atoms. Seel[10] has also shown in his systems that the chemical shift of axial fluorine atoms changes much more with changing temperature than is the case for the equatorial fluorines. For $CF_3SF_2SCF_3$, the chemical shift change for $-SF_2-$ is $\sim$4 ppm in the range -100 to 0°. We observe a chemical shift of $\sim$1–2 ppm over the same temperature range for $CF_3SF_2CF_3$ and $CF_3SF_2C_2F_5$. The peaks are sharp and well resolved at room temperature; there is some line broadening at the temperatures near -100°. We cannot say if the broadening indicates an exchange process like those described above or perhaps an internal rotation barrier. But an intramolecular axial–equatorial exchange seems unlikely. In c-$C_4F_8SF_2$, the S–F chemical shift is the same as for other $R_fR_f'SF_2$ compounds, but the rigid cyclic structure should preclude axial–equatorial exchange. Thus, the intermediate position of the $R_fR_f'SF_2$ shifts is more likely due to a change in chemical environment arising from the presence of the second R_f group. The temperature dependence of the chemical shift indicates a basically axial position. These axial fluorine atoms could still undergo intermolecular exchange. Preliminary examination of the Raman and infrared spectra of these $-SF_2-$ compounds, also, supports an axial arrangement of the fluorine atoms bonded to sulfur. This work will be reported subsequently. Thus, the sulfur–fluorine atoms in $CF_3SF_2CF_2CF_3$ are most likely in the axial positions having identical chemical shifts but having nonidentical coupling interactions with the geminal fluorine atoms of the vicinal methylene group.

The sharpness of the spectral lines at room temperature indicates that the barrier to rotation about the F_2C-SF_2 bond will be small so free rotation occurs. As noted above, the effect of a barrier may be appearing at low temperatures. Thus, there is chemical equivalence between the two fluorines of $-SF_2-$ and between the two fluorines of $-CF_2-$. The magnetic nonequivalence arises from the fact that the relationship between SF_A and CF_X (see below) does not average out to

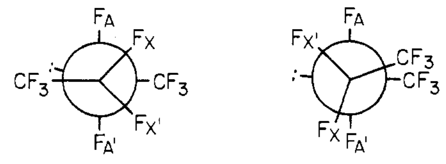

I II

be the same as between SF_A and CF_X', making $J_{AX} \neq J_{AX'}$. In rotamer I, F_A is cis to F_X and S-CF_3 is trans to C-CF_3. But in II, with F_A cis to F_X', S-CF_3 is cis to C-CF_3. Therefore, F_A does not perceive F_X' in II in the same way as F_A perceives F_X in I, although the relationship between the fluorines is cis in each case.

Acknowledgment. Fluorine research at the University of Idaho is supported by the National Science Foundation and the Office of Naval Research. We are grateful to Mr. C. Srivanavit for running some of the ^{19}F NMR spectra and to Professor C. D. Cornwell for helpful discussions.

Registry No. $CF_3SF_2CF_2CF_3$, 31222-06-7.

References and Notes

(1) Alfred P. Sloan Foundation Fellow, 1970–1972.
(2) H. M. McConnell, A. D. McLean, and C. A. Reilly, *J. Chem. Phys.*, **23**, 1152 (1955).
(3) D. T. Sauer and J. M. Shreeve, *J. Fluorine Chem.*, **1**, 1 (1971–1972).
(4) J. W. Emsley, J. Feeney, and L. H. Sutcliffe, "High Resolution Nuclear Magnetic Resonance Spectroscopy", Vol. I, Pergamon, New York, N.Y., 1965, pp 392–399.
(5) E. W. Lawless and L. D. Harmon, *J. Inorg. Nucl. Chem.*, **31**, 1541 (1969).
(6) E. L. Muetterties, W. Mahler, K. J. Packer, and R. Schmultzler, *Inorg. Chem.*, **3**, 1298 (1964); R. M. Rosenberg and E. L. Muetterties, *ibid.*, **1**, 756 (1962).
(7) C. T. Ratcliffe and J. M. Shreeve, *J. Am. Chem. Soc.*, **90**, 5403 (1968).
(8) T. Abe and J. M. Shreeve, *J. Fluorine Chem.*, **3**, 17 (1973–1974).
(9) R. A. Frey, R. L. Redington, and A. L. K. Aljibury, *J. Chem. Phys.*, **54**, 344 (1971).
(10) W. Gombler and F. Seel, *J. Fluorine Chem.*, **4**, 333 (1974).

Contribution No. 5008 from the Arthur Amos Noyes Laboratory of Chemical Physics, California Institute of Technology, Pasadena, California 91125

Proton Affinity and Gas-Phase Ion Chemistry of Hydrogen Fluoride

MICHAEL S. FOSTER and J. L. BEAUCHAMP*[1]

Received October 29, 1974

AIC40757D

The gas-phase ion chemistry of HF is investigated using the techniques of ion cyclotron resonance spectroscopy. The only observed reaction of the parent ion is $HF^+ + HF \rightarrow H_2F^+ + F$ for which a bimolecular rate constant $k = (9 \pm 3) \times 10^{-10}$ cm^3 molecule^{-1} sec^{-1} is determined. Proton-transfer reactions in mixtures of HF with N_2, CH_4, and CO_2 are examined to determine the proton affinity of HF. While HF is found to be substantially less basic than CH_4 and CO_2, the proton affinities of HF and N_2 are comparable. From the measured equilibrium constant and estimated entropy change a value of $\Delta H = -1.1 \pm 0.2$ kcal/mol is calculated for the reaction $H_2F^+ + N_2 \rightleftarrows N_2H^+ + HF$. From previous studies of PA(N_2) this allows an absolute value of PA(HF) = 112 ± 2 kcal/mol to be determined. The disparate base strength of HF relative to the other hydrogen halides is discussed.

I. Introduction

The proton affinity of a species M, defined as the enthalpy change for reaction 1, represents a quantitative measure of

$$MH^+ \rightarrow M + H^+ \quad \Delta H = PA(M) \tag{1}$$

the intrinsic basicity of the molecule in the gas phase. For two species M_1 and M_2, a knowledge of the preferred direction of the proton-transfer reaction 2 establishes the sign of the free

$$M_1H^+ + M_2 \rightleftarrows M_2H^+ + M_1 \tag{2}$$

energy change for the reaction, ΔG. If reaction 2 describes a system at thermal equilibrium, then the measured equilibrium constant gives ΔG according to $\Delta G = -RT \ln K$. Provided the entropic contribution $T\Delta S$ is also known, ΔH for reaction 2 is easily determined and gives directly the relative proton affinities of M_1 and M_2, i.e., $\Delta H = PA(M_1) - PA(M_2)$. An absolute measurement of either $PA(M_1)$ or $PA(M_2)$ then automatically gives the other.

The proton affinities of all the first- and second-row binary hydrides have been determined, with the notable exception of hydrogen fluoride. While several theoretical calculations of PA(HF) have appeared,[2,3] to our knowledge no experimental measurements of this quantity have been reported. This paper describes an ion cyclotron resonance (ICR) study of proton-transfer reactions occurring in mixtures of HF with several other molecules. Recently developed ICR trapped-ion techniques are employed in this study and permit evaluation of a proton-transfer equilibrium (eq 2) involving H_2F^+. The basicity thus derived for hydrogen fluoride illustrates again the frequently disparate behavior of fluorine relative to the other halogens.

II. Experimental Section

The theory and instrumentation of ICR spectroscopy have been previously described in detail.[4] The ICR trapped-ion technique has been discussed by McMahon.[5] Basically, an electron beam is momentarily pulsed to high energy (70 eV in these experiments) to produce ions from a low pressure of sample gas (typically 10^{-6} Torr). The ions are stored in the source region of the ICR cell where many collisions with neutral species may result in ion–molecule reaction products. After a predetermined and variable length of time, the ions are sampled and mass analyzed using ICR detection.[4,5] The application of this technique to measuring equilibrium constants has been described.[6,7]

In view of the expected propensity of hydrogen fluoride to attack the rhenium filament, HF pressures were kept less than 2×10^{-6} Torr, except during pressure calibration. Even at these low pressures, HF appeared to have deleterious effects on the trapping efficiency of the "flat" ICR cell used, somewhat increasing the normal rate of diffusive ion loss. Particularly adverse effects on the Schulz–Phelp ion gauge were observed during pressure calibration,[6] when the HF pressure appproached 10^{-3} Torr. In addition, the MKS Baratron Model 90H1-E capacitance manometer used to calibrate the ion gauge displayed greater-than-normal drift during this procedure. While the usual error in absolute pressure determination is estimated as $\pm 10\%$, in the case of HF limits of $\pm 30\%$ are more realistic.

Hydrogen fluoride (claimed to be anhydrous) was obtained from both Matheson Gas Products and Air Products and Chemicals. Samples were prepared and stored in stainless steel sampling cylinders, which were attached directly to the all-stainless inlet system. Low-pressure ICR spectra always showed the presence of water in the spectrum and H_2O^+ was frequently as much as 20% of the total ionization. Conditioning the inlet system by allowing HF to flow through it was usually successful in reducing the H_2O^+ intensity to <5% of the total, which is approximately the amount of water present during all of the equilibrium measurements.

III. Results and Discussion

The only observed reaction of the parent ion is process 3

$$HF^+ + HF \rightarrow H_2F^+ + F \qquad (3)$$

leading to protonated HF. A trapped-ion study[5] of HF shows the expected exponential decrease in HF^+ with time and the concomitant increase in H_2F^+. Several determinations of the rate constant for reaction 3 yield the value $(9 \pm 3) \times 10^{-10}$ cm^3 $molecule^{-1}$ sec^{-1}, the error estimate reflecting the uncertainty in absolute pressure. The rate coefficient calculated for eq 3 from the Langevin induced-dipole polarization theory[8] is 6.6×10^{-10} cm^3 $molecule^{-1}$ sec^{-1}, which is within the estimated experimental uncertainty range. Both the locked-dipole approximation[9] and the average dipole orientation treatment of Su and Bowers[9] give rate constants substantially larger than observed, 6.0×10^{-9} and 2.0×10^{-9} cm^3 $molecule^{-1}$ sec^{-1}, respectively. Since the latter analysis often predicts rate constants for polar systems fairly closely, it appears that

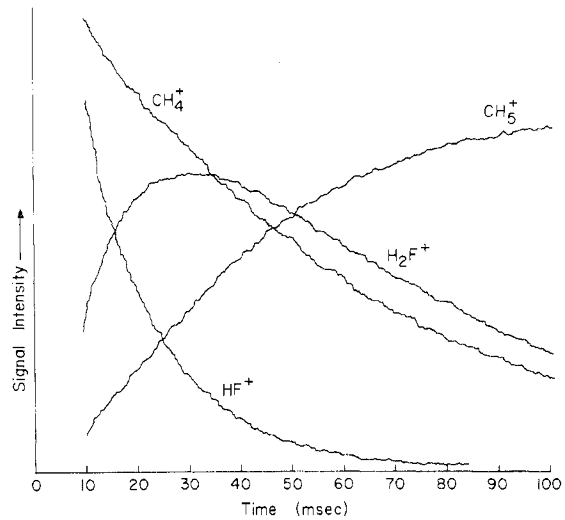

Figure 1. Variation with time of positive ion intensities following a 5-msec, 70-eV electron beam pulse in a 1:1 mixture of HF and CH_4 at 1×10^{-6} Torr. For clarity, CH_3^+ and $C_2H_5^+$ are not shown.

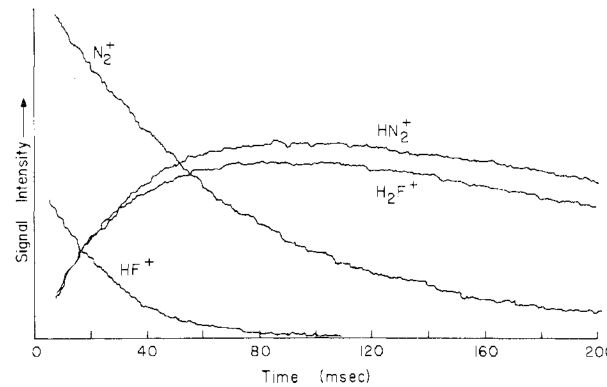

Figure 2. Variation with time of positive ion intensities following a 4-msec, 70-eV electron beam pulse in a 2.5:1 mixture of HF and N_2 at 1×10^{-6} Torr.

reaction 3 does not occur on every collision.

Proton-transfer reactions involving hydrogen fluoride were examined in binary mixtures of HF with CH_4, CO_2, and N_2. The variation of ion intensities with time following a 5-msec, 70-eV electron beam pulse in a 2:1 mixture of HF and CH_4 is shown in Figure 1. The temporal variation of ion concentrations along with double-resonance experiments show the expected reactions of the primary ions, eq 3–5. The decline

$$CH_4^+ + CH_4 \rightarrow CH_5^+ + CH_3 \qquad (4)$$

$$HF^+ + CH_4 \rightarrow H_2F^+ + CH_3 \qquad (5)$$

with time of H_2F^+ with respect to CH_5^+ in Figure 1 suggests the occurrence of reaction 6, which was also verified by double

$$H_2F^+ + CH_4 \rightarrow CH_5^+ + HF \qquad (6)$$

resonance. The reverse of process 6 could not be detected. The conclusion is that $PA(CH_4) > PA(HF)$.

Mixtures of HF with CO_2 showed an analogous sequence of reactions and the ion intensity curves resembled those of Figure 1. The proton-transfer reaction 7 was observed but

$$H_2F^+ + CO_2 \rightarrow CO_2H^+ + HF \qquad (7)$$

not its reverse, implying that $PA(CO_2) > PA(HF)$.

A similar experiment with nitrogen produced the results of Figure 2, which shows the variation with time of ion intensities in a 2.5:1 mixture of HF and N_2 at 1×10^{-6} Torr. In this case, the relative abundances of H_2F^+ and HN_2^+ remain constant with time out to 200 msec. Ejection of either HN_2^+ or H_2F^+ in double-resonance experiments leads to the decay of the remaining ion, indicating that reaction 8 proceeds

$$H_2F^+ + N_2 \rightleftharpoons HN_2^+ + HF \tag{8}$$

reversibly. The gradual decrease with time of both ions reflects diffusive ion loss (which is slightly faster for the lighter H_2F^+)[10] and also reaction with the H_2O impurity to form H_3O^+.

Since reaction 8 is observed to proceed in both directions, the relatively constant ratio of the HN_2^+ and H_2F^+ ion intensities in Figure 2 is interpreted as reflecting an equilibrium situation. From the known ratio of neutral pressures and the measured ratio of ion abundances (derived from Figure 2 by dividing ion intensity by ion mass), the equilibrium constant for eq 8 is determined as 2.0 ± 0.6. Over a period of 18 months, four independent measurements of the equilibrium constant gave results of 2.0 ± 0.6, 4.0 ± 1.2, 2.7 ± 0.8, and 4.5 ± 1.4. Owing to the difficulty in pressure measurement the spread in these data is worse than usually encountered. The average of these values gives $K = 3.3 \pm 1.0$ and $\Delta G = -0.7 \pm 0.2$ kcal/mol for reaction 8 as written.

The entropy contribution to reaction 8, knowledge of which is necessary to extract ΔH, can be estimated by assuming the entropies of the ionic species to be equal to those of the isoelectronic neutrals, i.e., $S(HN_2^+) = S(HCN)$ and $S(H_2F^+) = S(H_2O)$. With this assumption, $T\Delta S = -0.36$ kcal/mol for eq 8, yielding $\Delta H = -1.1 \pm 0.2$ kcal/mol.[11] Thus, the proton affinity of nitrogen is greater than that of hydrogen fluoride by this amount.

The proton affinities of methane and carbon dioxide appear reasonably well established. $PA(CH_4)$ is 1.5 ± 0.1 kcal/mol higher than $PA(CO_2)$[12] and absolute values for both are approximately 127 kcal/mol.[13,14] Equations 6 and 7 thus provide essentially the same upper limit on the proton affinity of hydrogen fluoride: $PA(HF) < 127$ kcal/mol.

The proton affinity of nitrogen can be estimated by several methods. Observation of ion–molecule reactions brackets $PA(N_2)$ between 113 and 127 kcal/mol.[15] The theoretical calculation of 118 ± 3 kcal/mol by Forsen and Roos falls in this range.[16] With a flowing afterglow apparatus, Bohme and coworkers[17] have measured an equilibrium constant of $(9.3 \pm 4.0) \times 10^8$ for reaction 9. This corresponds to $\Delta G = -12.2$

$$H_3^+ + N_2 \rightleftharpoons HN_2^+ + H_2 \tag{9}$$

± 0.3 kcal/mol and from the entropies for H_3^+,[18] N_2,[11] HN_2^+ ($=$HCN),[11] and H_2,[11] $T\Delta S$ is calculated as -0.5 kcal/mol yielding $\Delta H = -12.7 \pm 0.3$ kcal/mol for reaction 9. Adopting a value of 100 ± 1 kcal/mol for $PA(H_2)$,[18-20] the proton affinity of nitrogen is estimated by this procedure to be 112.7 ± 1.3 kcal/mol. Bohme[21] has suggested 113.6 ± 1.6 kcal/mol for $PA(N_2)$. For the purpose of this discussion, a value of $PA(N_2) = 113 \pm 2$ kcal/mol will be adopted, and thus $PA(HF) = 112 \pm 2$ kcal/mol. This is in reasonably good agreement with the theoretical predictions of 108 kcal/mol[2] and 114 kcal/mol.[3]

This result provides an interesting comparison with the other hydrogen halides. Table I presents available proton affinity data for HX and CH_3X molecules (X = F, Cl, Br, I). Two relevant observations will be discussed: (1) the proton affinities of HI, HBr, and HCl are about the same, while PA(HF) is dramatically lower; (2) the methyl substituent effect on proton affinity, ΔPA in Table I, shows a marked reversal of trend between HCl and HF, and the effect for HF is very large.

The erratic behavior of the proton affinities of HX can be interpreted as resulting from the convolution of two opposite trends seen in the following analysis. The hydrogen affinity of an ion M^+, defined as the enthalpy change for reaction 10,

$$MH^+ \rightarrow M^+ + \dot{H} \tag{10}$$

represents the homolytic bond dissociation energy of MH^+ and is related to the proton affinity of M by expression 11. In Table I are presented the ionization potentials of the hydrogen

Table I. Proton Affinities, Hydrogen Affinities, and Ionization Potentials of Hydrogen Halides and Methyl Halides[a]

X	PA-(HX)	PA-(CH_3-X)[d]	ΔPA	IP(HX)	HA-(HX^+)	*D*-(X–H)	HA-(CH_3-X^+)[d]
I	145[b]	170	25	240[e]	71	71[g]	77
Br	141[b]	163	22	268[e]	95	87[g]	93
Cl	141[b]	160	19	294[e]	121	103[g]	107
F	112[c]	151	39	369[f]	167	136[f]	126

[a] All data in kilocalories per mole at 298°K. [b] M. A. Haney and J. L. Franklin, *J. Phys. Chem.*, 73, 4328 (1969). [c] This work. [d] J. L. Beauchamp, D. Holtz, S. D. Woodgate, and S. L. Patt, *J. Am. Chem. Soc.*, 94, 2798 (1972). [e] J. L. Franklin, J. G. Dillard, H. M. Rosenstock, J. T. Herron, K. Draxl, and F. H. Field, *Natl. Stand. Ref. Data Ser., Natl. Bur. Stand.*, No. 26. [f] Calculated from data in J. Berkowitz, W. A. Chupka, P. M. Guyon, J. H. Holloway, and R. Spohr, *J. Chem. Phys.*, 54, 5165 (1971). [g] Reference 11.

$$PA(M) = HA(M^+) - IP(M) + IP(H) \tag{11}$$

halides and the resultant $HA(HX^+)$ calculated with eq 11. Both IP(HX) and $HA(HX^+)$ increase monotonically proceeding from iodine to fluorine paralleling the behavior of the neutral hydrogen halide homolytic bond dissociation energies (Table I) as well as those for the isoelectronic neutrals.[4] According to eq 11, PA(HX) is related to the *difference* between $HA(HX^+)$ and IP(HX). Thus, the two progressions work in opposite directions and the approximately equal proton affinities of HI, HBr, and HCl result essentially from a cancelation effect. The exceptionally high ionization potential of HF, however, dominates $HA(HF^+)$ in expression 11, thus lowering PA(HF) drastically and accounting for the irregular sequence of HX proton affinities. Since $PA(CH_3X)$ exhibits a more orderly progression (Table I), this results in a very large methyl substituent effect for HF.[22] The large methyl substituent effect may also indicate that a special stabilization is afforded CH_3FH^+. Possible delocalized structures for this ion include I–III which would likely be more important for fluorine than for the remaining halogens.

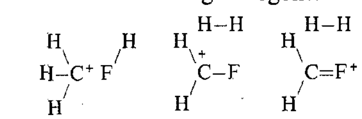

I II III

Finally, it is of interest to note that the lowest energy ionization process of the hydrogen and methyl halides, with the sole exception of methyl fluoride, involves removal of an electron from a nonbonding orbital localized largely on the halogen. In the case of methyl fluoride, ionization at threshold involves a removal of an electron from the π_e C–H σ-bonding orbital.[23] While this contrasting behavior is probably responsible for the low value of $HA(CH_3F^+)$ compared to trends for the remaining methyl halides, it leads to a stabilization of the radical ion rather than the conjugate acid of CH_3F and thus does not appear to be related to the large methyl substituent effect.

Acknowledgment. This research was supported in part by the United States Atomic Energy Commission under Grant No. AT(05-3) 767-8 and by the National Science Foundation under Grant No. NSF-GP-18383.

Registry No. HF, 7664-39-3; H_2F^+, 12206-67-6; CH_4, 74-82-8; CO_2, 124-38-9; N_2, 7727-37-9; HN_2^+, 12357-66-3.

References and Notes

(1) Dreyfus Teacher-Scholar, 1971–1976.
(2) A. C. Hopkinson, N. K. Holbrook, K. Yates, and I. G. Csizmadia, *J. Chem. Phys.*, **49**, 3596 (1968), and references to Table V therein.
(3) A. Johansson, P. A. Kollman, J. F. Liebman, and S. Rothenberg, *J. Am. Chem. Soc.*, **96**, 3750 (1974).
(4) J. L. Beauchamp, *Annu. Rev. Phys. Chem.*, **22**, 527 (1971).
(5) T. B. McMahon and J. L. Beauchamp, *Rev. Sci. Instrum.*, **43**, 509 (1972).

(6) R. J. Blint, T. B. McMahon, and J. L. Beauchamp, *J. Am. Chem. Soc.*, **96**, 1269 (1974).
(7) R. H. Staley and J. L. Beauchamp, *J. Am. Chem. Soc.*, **96**, 6252 (1974).
(8) G. Gioumousis and D. P. Stevenson, *J. Chem. Phys.*, **29**, 294 (1958).
(9) T. Su and M. T. Bowers, *Int. J. Mass Spectrom. Ion Phys.*, **12**, 347 (1973).
(10) T. E. Sharp, J. R. Eylar, and E. Li, *Int. J. Mass Spectrom. Ion Phys.*, **9**, 421 (1972).
(11) "JANAF Thermochemical Tables," *Natl. Stand. Ref. Data Ser., Natl. Bur. Stand.*, **No. 37** (1971).
(12) R. S. Hemsworth, H. W. Rundle, D. K. Bohme, H. I. Schiff, D. B. Dunkin, and F. C. Fehsenfeld, *J. Chem. Phys.*, **59**, 61 (1973).
(13) W. A. Chupka and J. Berkowitz, *J. Chem. Phys.*, **54**, 4256 (1971).
(14) M. A. Haney and J. L. Franklin, *Trans. Faraday Soc.*, **65**, 1794 (1969).
(15) A. E. Roche, M. M. Sutton, D. K. Bohme, and H. I. Schiff, *J. Chem. Phys.*, **55**, 5480 (1971).
(16) S. Forsen and B. Roos, *Chem. Phys. Lett.*, **6**, 128 (1970).
(17) D. K. Bohme, R. S. Hemsworth, H. W. Rundle, and H. I. Schiff, *J. Chem. Phys.*, **58**, 3504 (1973).
(18) M. E. Schwartz and L. J. Schaad, *J. Chem. Phys.*, **47**, 5325 (1967).
(19) J. A. Burt, J. L. Dunn, M. J. McEwan, M. M. Sutton, A. E. Roche, and H. I. Schiff, *J. Chem. Phys.*, **52**, 6062 (1970).
(20) A. J. Duben and J. P. Lowe, *J. Chem. Phys.*, **55**, 4270 (1971).
(21) D. K. Bohme, private communication.
(22) Basicity data for other systems (e.g., H_2O and CH_3OH, PH_3 and CH_3PH_2, etc.) reveal that the methyl substituent effect on proton affinity generally ranges between 15 and 20 kcal/mol (see ref 3). Thus, the effect in HF is exceptionally large compared with those of all of the other simple hydrides.
(23) D. W. Turner, "Molecular Photoelectron Spectroscopy", Wiley-Interscience, London, 1970. The value of IP(CH_3F) reported by Turner is somewhat in error. The hydrogen affinity of CH_3F^+ in Table I is calculated from PA(CH_3F) using IP(CH_3F) = 12.54 eV [B. P. Pullen, T. A. Carlson, W. E. Moddeman, G. K. Schweitzer, W. E. Bull, and F. A. Grimm, *J. Chem. Phys.*, **53**, 768 (1970)]. The lowest IP corresponds to the π_e orbital; recent experiments suggest that the σ_{a_1} and $2p\pi$ orbitals are observed at ~13.3 and ~16.5 eV, respectively [T. A. Carlson, G. E. McGuire, A. E. Jonas, K. L. Cheng, C. P. Anderson, C. C. Lu, and B. P. Pullen, *Electron Spectrosc., Proc. Int. Conf.*, 207 (1972)].

Contribution from the Chemistry Department, Colorado State University, Fort Collins, Colorado 80523

Dissociative Chlorination of Nitrogen Oxides and Oxy Anions in Molten Sodium Chloride–Aluminum Chloride Solvents

R. J. GALE and R. A. OSTERYOUNG*

Received September 20, 1974 AIC406634

Nitrosyl cation has been found to undergo reversible one-electron reduction–oxidation in molten NaCl–$AlCl_3$ mixtures (175°) at vitreous C electrodes. The NO^+ ion half-wave potential in normal pulse voltammograms occurs at $E_{1/2} \approx +1.86$ V vs. Al reference electrode in $NaAlCl_4$(NaCl saturated) and a diffusion coefficient for NO^+ ion in acidic melts ($AlCl_3$ rich) is estimated to be 1.8×10^{-5} cm^2 sec^{-1} (175°). Nitrite ion reacts with fused NaCl–$AlCl_3$ mixtures to produce high yields of NO^+ ion, which is separable from the solvent phase as nitrosyl chloride. Nitryl ion, nitrogen dioxide, and nitrate ion are reduced in these molten salts, to varying extents, whereas nitrous oxide and nitric oxide remain unaffected in 24 hr. Possible mechanisms are discussed for these dissociative chlorination processes.

Introduction

Interpretations of potentiometric data[1-6] and of Raman spectral data[7] with ionic equilibria models have advanced the understanding of the structures of molten alkali metal chloride–aluminum chloride mixtures. Their acid–base characteristics, using Lux–Flood theory terminology, vary with both the alkali metal chloride:aluminum chloride molar ratio and the nature of the alkali metal cation. These chloroaluminate solvents are known to be effective chlorinating agents for a number of oxides and oxy anions,[8-12] e.g., H_2O, TiO_2, TiO_3^{2-}, GeO_2, GeO_3^-, As_2O_3, AsO_2^-, SnO_2, SnO_3^{2-}, and Sb_2O_5. In this regard, they behave similarly to aluminum chloride in its high-temperature (150–500°) reactions with many oxygen-containing compounds[13-18] (e.g., MgO, γ-AlOOH, γ-Al_2O_3, SO_2, CaO, TiO_2, V_2O_5, Fe_2O_3, FeOCl, ZnO, As_2O_3, Nb_2O_5, $NbOCl_3$, MoO_3, Sb_2O_5, Sb_2O_3, Ta_2O_5, and Bi_2O_3). Aluminum oxychloride and the corresponding chlorides or oxychlorides are obtained as products, e.g.

$$2H_2O + Al_2Cl_6 \xrightarrow{\Delta} 2AlOCl + 4HCl$$

$$WO_3 + Al_2Cl_6 \xrightarrow{\Delta} 2AlOCl + WOCl_4$$

In this study, selected nitrogen oxides and oxy anions have been allowed to react with NaCl–$AlCl_3$ melts at 175° to examine further the chlorination capabilities of these fused-salt media. Chemical analysis and electroanalytical techniques were used in conjunction to identify the major intermediates and products of reactions.

Experimental Section

Chemicals. Matheson gases nitric oxide (CP grade), chlorine (Research grade), nitrosyl chloride (97% minimum purity), and nitrogen dioxide (99.5% minimum purity) were redistilled several times before being weighed and condensed in reaction vessels. Sodium tetrachloroaluminate melt preparation, purification, and analysis methods were similar to those described in earlier publications.[19,20] To obtain samples of sodium tetrachloroaluminate for vacuum-line experiments, the molten salt was filtered through a fritted-glass disk into a Pyrex tube to remove any aluminum particles which readily dislodge from the cathode during and after melt purification. Sodium nitrite (Baker Analyzed) and sodium nitrate (Mallinckrodt, analytic) were stored in a desiccator over P_2O_5, in the drybox. Nitrosyl and nitryl tetrafluoroborates (Research Organic/Inorganic Chemical Corp.) and nitrous oxide gas (98.0% minimum purity) were used as supplied. Air-sensitive compounds always were handled under vacuum or dried nitrogen atmospheres.

Apparatus. Volatile products were condensed from the reaction vessels in cold traps at liquid nitrogen temperature. Subsequently, the condensates could be analyzed conveniently by infrared spectroscopy and/or gas chromatography of the gaseous constituents. Solid reactants in glass vials were added from side arms and gases were introduced into the reaction vessels, after vacuum degassing the $NaAlCl_4$ melts. Suitable glassware was heated to 500° for several hours immediately before being transferred into the drybox. Vacuum joints were coated lightly with Dow Corning Silicone High Vacuum grease. Quantitative ir spectral data were collected on a Beckman IR 12 spectrophotometer operated in the single-beam mode. For calibration and analysis purposes, gases were expanded into a 5-cm glass cell fitted with Irtran-2 plates (Barnes Engineering Co.); a linear Beer–Lambert plot of the $2\nu_1$ band center (3563.3 cm^{-1} [21]) was obtained for nitrosyl chloride gas pressures in the experimental range. Nitric oxide, nitrous oxide, and chlorine were analyzed on a Carle Model 8000 gas chromatograph, fitted with a mini single-loop sampling valve and a Polypak 1 column (3 ft × 1/8 in. o.d., S/S), which was operated at ambient temperatures with He carrier gas (20 psi).[22] The apparatus used for the uv measurement was similar to that previously described.[23] Samples of solidified melts were extracted with liquid sulfur dioxide to remove the soluble $NaAlCl_4$, using the